Raman spectrum of solid nitrogen at high pressures and low temperatures*

F. D. Medina† and W. B. Daniels

Department of Physics, University of Delaware, Newark, Delaware 19711
(Received 20 January 1975)

The Raman spectrum of solid nitrogen has been studied at high pressures and low temperatures using a method of sample preparation that allows the separation of effects due to change of molar volume and of temperature, respectively. Two lines have been observed in the lattice region of the γ phase which are identified as E_g and B_{1g} librational modes on the basis of frequency and relative intensity calculations. An asymmetrical line has been observed in the stretching region of this phase. In the α phase, the measured Grüneisen parameters indicate that neither the quadrupolar nor the 6–12 atom–atom interaction potential has the correct volume dependence. The temperature dependence of the frequency and linewidth of the E_g librational mode is proposed to be due to libron–phonon interactions. Two very broad Raman lines are observed in the lattice region of the β phase. The low- and high-frequency lines are identified with translational and librational modes, respectively. The observations are consistent with a precessing molecule model for the β phase.

I. INTRODUCTION

Considerable experimental and theoretical work has been devoted to molecular solids, such as H_2, N_2, CO, CO_2, CH_4, and others. These solids represent the first step in complexity from the monatomic inert gases. They are among the simplest systems where one can study molecular rotations, i.e., where one can study the anisotropic or orientation-dependent part of the intermolecular potential. Some of these solids are also of interest because they exhibit phase transitions which presumably are associated with the anisotropic part of the intermolecular potential.

Solid nitrogen exhibits such a transition from an orientationally ordered phase at low temperatures to a highly orientationally disordered phase at high temperatures. This transition has been shown to be from a cubic α phase to a hexagonal β phase, as the temperature is increased.[1–11] Another phase, the high pressure γ phase,[12,13] has been found to have a tetragonal structure.[14]

The nitrogen phase diagram is shown in Fig. 1. This diagram covers the temperature range from 0 to 200 °K and the molar volume range from 23.37 to 27.81 cm^3/mole, and includes the fluid, vapor, and three solid phases of nitrogen. The transition lines between the different phases and isobars every 1kbar up to 6 kbar are also shown in this figure. This figure has been partly constructed from a similar figure in Ref. 6. More recent data on the melting parameters[15] and the relative length changes along the solid–vapor line[16] of nitrogen have been used to construct the melting and solid–vapor lines. In addition, the α–β–γ triple point of solid nitrogen used in Fig. 1 has been estimated from the results of nuclear quadrupole resonance studies of the α–β transition.[17]

Studies on the structure of the α phase favor either a $Pa3(T_h^6)$ or a $P2_13(T^4)$ space group. The $Pa3$ structure has four molecules per unit cell with the molecular centers arranged in a face-centered cubic lattice and the molecular axes oriented along one of the four cube diagonals. In the $P2_13$ structure the molecules are displaced along the cube diagonals from the center of inversion symmetry they occupy in the $Pa3$ structure.

The experimental evidence supporting each structure is extensive. In some x-ray[2,3,6] and electron[8–11] diffraction experiments lines which are forbidden for the $Pa3$ structure were not detected. The $Pa3$ structure is further supported by measurements of the optical birefringence that indicate cubic symmetry[18] and the absence of coincidences between the frequencies in the Raman spectrum[19–23] and the infrared absorption spectrum.[24–28] In other x-ray diffraction experiments[1,4,7] lines which are forbidden for the $Pa3$ structure were observed. Further support for the $P2_13$ structure is provided by the detection of piezoelectric resonances[27] and a Raman-active line in the infrared absorption spectrum,[28] since neither is allowed in the centrosymmetric $Pa3$ structure. From an analysis of their data, Jordan *et al.*,[5] and LaPlaça and Hamilton[7] estimate the displacement of the nitrogen molecules from their centers of symmetry to be 0.17 and 0.16 Å, respectively. However, the electron diffraction data of Venables and English[11] can establish an upper limit of 0.05 Å for this displacement. Furthermore, these authors argue that the measurements supporting the $P2_13$ structure can be explained by the presence of twins and other defects.[11]

Finally, the stability of the $Pa3$ structure has been established using different methods and intermolecular potentials.[29–35] In particular, Goodings and Henkelman[35] used the Kohin potential[30] in a classical calculation of the crystal energy as a function of the displacement of the nitrogen molecules along the cube diagonals and found that the lowest energy corresponds to zero displacement or, in other words, the $Pa3$ structure. More recently, Zunger and Huler[36] used the so-called 6–12 atom–atom potential and again determined $Pa3$ as the more stable structure.

Assuming the $Pa3$ structure for the α phase, two stretching modes of symmetry A_g and T_g, and three librational modes of symmetry E_g, T_g, and T_g, are expected in the first-order Raman spectrum. Two translational modes of symmetry T_u are infrared-active.

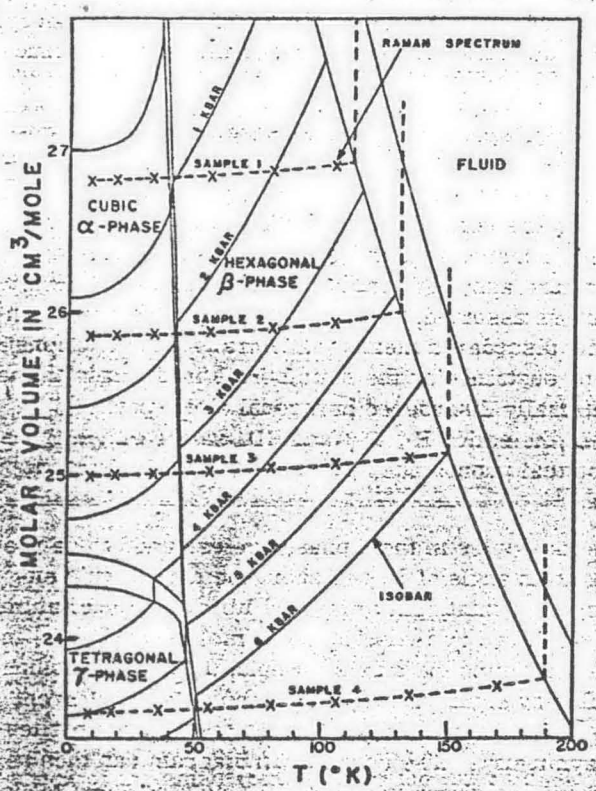

FIG. 1. Nitrogen phase diagram partly reproduced from Ref. 6 and more recent data from Refs. 15–17.

Coincidences between Raman and infrared frequencies are not allowed. The Raman spectrum for the α phase has been measured by several workers,[19–23] who obtained librational frequencies which differ by as much as 6%. Four lines have been observed in the lattice region: Three relatively narrow lines which have been assigned to the librational modes and a very broad band around 80 cm^{-1}. In the stretching region two lines with a separation of about 1.2 cm^{-1} have been reported.[21] As the temperature is increased from below 20 °K to just below the α–β transition temperature, the librational frequencies decrease by as much as 15% and the lines broaden considerably.[19,20,22] This temperature dependence of the Raman frequencies and linewidths must be ascribed to anharmonicities. The anharmonicities result from large librational and translational amplitudes. The anomalous increase in the linear coefficient of thermal expansion[16,37] and the heat capacity,[38] and the temperature dependence of the nuclear quadrupole resonance frequency[39] have also been ascribed to large librational amplitudes.[16,39] The rms librational amplitudes calculated from Raman[20] and nuclear quadrupole resonance[17] data range from 14° at 16 °K to 19° near the α–β transition temperature.

The librational frequencies in the α phase have also been the subject of an impressive number of classical and quantum mechanical calculations aimed at elucidating the form of the anisotropic part of the intermolecular potential.[21,34–36,40–49] Several anisotropic potentials have been used in these calculations: quadrupolar, Kohin, and atom–atom interaction potentials. The quadrupolar potential has an r^{-5} dependence on the intermolecular distance r. The Kohin potential adds anisotropic dispersive and repulsive interactions having r^{-6} and r^{-12} dependence, respectively. The atom–atom potential consists of 6–12 interactions between nonbonded atoms.

Quantum mechanical calculations using the quadrupolar interaction potential give the best agreement with the measured librational frequencies.[43–47] Monte Carlo studies of classical free rotors using the quadrupolar interaction potential[48] give good agreement with several experimental quantities. However, a quadrupole-induced mechanism gives poor results for the infrared intensities.[28] Furthermore, the Kohin potential is needed to obtain good agreement between the calculated crystal energy and the measured sublimation energy.[30,35] Unfortunately, classical[35] and quantum mechanical[45] calculations with the Kohin potential yield librational frequencies which are as much as 90% and 50% larger than the measured frequencies, respectively. The general conclusion is that either the forms or the relative strengths of the different terms in the Kohin potential are incorrect.[45]

The atom–atom potential has also been used extensively to calculate librational frequencies and other properties of the α phase.[34,36,40,41,47,49] This potential has yielded good agreement with many experimental properties. Jacobi and Schnepp[47] used a 6–n atom–atom potential and obtained best agreement with experimental properties for $n=9$. Zunger and Huler[36] have studied the effect of zero-point energy and complete relaxation of forces and torques on the properties of α-N_2, while Raich, Gillis and Anderson[49] have studied the temperature dependence of the librational and translational lattice modes using the self-consistent phonon approximation. Although both studies are moderately successful in fitting observed properties, the authors conclude that a more complete potential is needed. More recently, Mandell[50] proposed an anisotropic intermolecular potential consisting of a sum of multipolelike interactions and concluded that terms of hexadecapolar symmetry play a significant role in the orientational properties of α-N_2 and that these terms are weak in the 6–12 atom–atom potential. Another criticism of calculations using the atom–atom potential is the introduction of a "new parameter," the bond length of the nitrogen molecule, which can then be adjusted to give best agreement with experiment.

The structure of the high pressure γ phase is tetragonal with a $P4_2/mnm(D_{4h}^{14})$ space group and two molecules per unit cell.[14] The molecules are arranged in layers with the molecular axes parallel within a layer and perpendicular in adjacent layers, as shown in Fig. 2. For a molar volume of 24.09 cm^3/mole, x-ray diffraction experiments give lattice constants $a=3.957$ Å and $c=5.109$ Å.[14] The correlation diagram of the γ phase at the center of the Brillouin zone derived from group theoretical considerations[51] is shown in Table I. The numbers in parenthesis indicate the number of modes of that symmetry. The librational and translational modes are separable at the zone center. Two stretching modes of symmetry A_{1g} and B_{2g}, and two librational modes of symmetry B_{1g} and E_g, are expected in the first-order Raman spectrum. One translational mode of symmetry

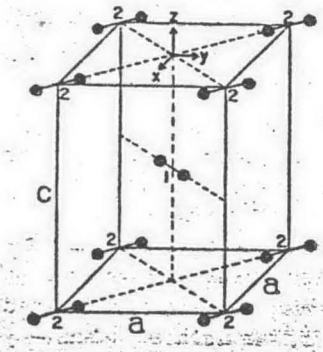

FIG. 2. Unit cell of the γ phase determined by x-ray diffraction experiments in Ref. 14.

D_{4h}^{14} STRUCTURE

E_u is infrared active. Coincidences between Raman and infrared frequencies are not allowed. The Raman spectrum of the γ phase has been previously reported.[23] Two lines were observed in the lattice region.

At the higher densities corresponding to the γ phase the anisotropic intermolecular potential is likely to be more harmonic and to contain a larger contribution from the repulsive interaction. However, neither the quadrupole, nor the Kohin, nor the 6–12 atom–atom potential is capable of explaining the stability of the D_{4h}^{14} structure.[33,36,52] Raich and Mills[52] showed that a Kohin potential where the repulsive term is replaced by a shape-dependent hard-core potential, similar in shape to the calculated electron distribution, accounts for the stability of the γ phase. Finally, Mandell[50] has shown that hexadecapolar terms in the multipolelike expansion of the intermolecular potential can account for the α to γ transition.

X-ray diffraction studies of the β phase indicate that the molecular centers are arranged in a hexagonal closed-packed structure[2–6] with a high degree of orientational disorder. The molecular axes are inclined at an angle of about 56 deg with respect to the crystal c axis.[5–6] Calculations using the quadrupolar[42,48,52] and 6–12 atom–atom[53] interaction potentials can predict a first-order transition from the orientationally ordered α phase to an orientationally disordered phase at higher temperatures. The x-ray diffraction data is equally well fit by having the molecules precessing about the c axis or randomly distributed among the 24 general positions of space group $P6_3/mmc$ (D_{6h}^4). Schuch and Mills[6] analysed the packing of nitrogen molecules assuming their surface to be defined by the 0.002 electron density contour. They found that the molecules overlap slightly and can not precess freely about the c axis but can take the random orientations of space group $P6_3/mmc$ without overlapping. The c to a ratio has been found to be close to the ideal value of 1.633 for closest packing of hard spheres.[3–6] However, molecular volume data,[3] estimates of the rotational specific heat[54] and the entropy,[55] and the detection of a small but nonzero nuclear quadrupole coupling constant,[56] rule out completely free rotation. The results of the nuclear quadrupole resonance experiments are consistent with the molecules being aligned at an angle of 54.7 deg with respect to the c axis while precessing or jumping among different positions at a rate fast compared to the resonance frequency. These results also rule out the randomly oriented structure.

The Raman spectrum of the β phase in the lattice region has been reported to resemble the wing of the Rayleigh line, whereas in the stretching region a single line with wings has been observed.[20] The Raman spectrum expected on theoretical grounds depends obviously on the structure assumed for the β phase. If the $P6_3/mmc$ structure is assumed, the fact that molecules are orientationally disordered means that librational excitations cannot be sustained by the solid. This is the case in the orientationally disordered hexagonal close-packed phases of the solids H_2, D_2, and HD, where only a transverse optical phonon has been observed in the Raman spectra.[57]

If the molecules in the β phase are assumed to be precessing at an angle of 56 deg about the c axis, this entails some orientational order and librational excitations can be sustained by the solid. The molecules librate in a plane containing the c axis. Replacing the precessing molecules by some "average" molecules with different polarizability, these new molecules are sitting on sites of D_{3h} symmetry. The correlation diagram can then be worked out, as shown in Table II. One stretching mode of symmetry A_{1g}, one librational mode of symmetry E_{1g}, and one translational mode of symmetry E_{2g}, are expected in the first-order Raman spectrum. None of the modes are infrared-active.

It should be clear from the previous discussions that many questions about solid nitrogen are still unanswered. The most fundamental concern is the form of the anisotropic part of the intermolecular potential. Some detailed subjects of interest are: (1) The structure of the α phase; (2) the Raman spectrum of the β phase; (3) the structure of the β phase; (4) the Raman spectrum of the γ phase; (5) anharmonicities of all solid phases, and others. The present study of the Raman spectrum of

TABLE I. Correlation diagram for the γ phase at the center of the Brillouin zone.

Molecular symmetry $D_{\infty h}$	Site symmetry D_{2h}	Factor group symmetry D_{4h}	Activity
$\Sigma_g^+(\nu)$	A_g	$A_{1g}(1)$	Raman (1)
		$B_{2g}(1)$	Raman (1)
$\Sigma_u^+(T_z)$	B_{2u}	$E_u(2)$	ir(1), acoustic (1)
$\pi_u(T_x, T_y)$	B_{3u}	$B_{1u}(1)$	...
	B_{1u}	$A_{2u}(1)$	acoustic (1)
$C_\infty - C_2(x)$			
$\pi_g(R_x, R_y)$	B_{1g}	$B_{1g}(1)$	Raman (1)
	B_{3g}	$A_{2g}(1)$	...
$C_\infty - C_2(y)$			
$\pi_g(R_x, R_y)$	B_{1g}		
	B_{2g}	$E_g(1)$	Raman (1)

TABLE II. Correlation diagram for the β phase at the center of the Brillouin zone.

Molecular symmetry $D_{\infty h}$	Site symmetry D_{3h}	Factor group symmetry D_{6h}	Activity
$\Sigma_g^+(\nu)$	A_1'	$A_{1g}(1)$	Raman (1)
		$B_{1u}(1)$	...
$\pi_g(R_x, R_y)$	E''	$E_{1g}(1)$	Raman (1)
		$E_{2u}(1)$	Acoustic (1)
$\Sigma_u^+(T_z)$	A_2''	$B_{2g}(1)$	...
		$A_{2u}(1)$	Acoustic (1)
$\pi_u(T_x, T_y)$	E'	$E_{2g}(1)$	Raman (1)
		$E_{1u}(1)$	...

solid nitrogen at various temperatures and pressures was undertaken with the hope of shedding light on some of these questions.

The experimentally measured quantities serve as a check of the anisotropic part of the intermolecular potential used in a particular theory. Pressure dependence studies can provide a severe test for any theory. This is particularly true since most infrared and Raman experiments on nitrogen have been done along the solid–vapor line, the exception being the Raman scattering experiments of Thiery *et al.*, recently reported.[23] However, these experiments were done at only one temperature and under nonhydrostatic pressure that made quantitative results less reliable. The present high pressure experiments are unique because of the use of a novel method of sample preparation that allows the separation of temperature and volume effects on the Raman spectrum. This is accomplished by constraining the sample inside a high pressure optical cell and hence assuring that the molar volume changes only slightly as the temperature is lowered.

In the present work the experimental techniques used in obtaining Raman spectra of the three known phases of solid nitrogen are described. Results for the three phases are presented. Calculations of the librational frequencies and relative intensities are compared to the experimental results in the γ phase. The volume dependence of the Raman frequencies in the α phase is discussed in relation to the form of the anisotropic part of the intermolecular potential within the context of the quasiharmonic approximation. The temperature dependence of the Raman spectrum is discussed in relation to the cubic and quartic anharmonic terms in the Hamiltonian of a perturbative treatment of the lattice dynamics of the α phase. Finally, the Raman spectrum of the β phase is discussed and its structure is identified.

Preliminary reports on the Raman spectrum of the γ phase and the volume dependence of the Raman frequencies in the α phase have already appeared in the literature.[58,59]

II. EXPERIMENTAL DETAILS

Samples used in Raman scattering studies are usually grown by condensation from the gas phase on a substrate. This method has several disadvantages: (1) Strains are usually present in the samples during growth, leading to sample cracking and defects and the resultant loss of optical quality; (2) the external surfaces are of poor optical quality; and (3) as the temperature of the sample is changed, changes in the frequencies of the Raman lines result from changes in both temperature and volume. These effects cannot be separated in a single such experiment.

The experimental method used in this work remedies the above mentioned disadvantages. Samples of solid nitrogen are prepared by growth within an optical cell at high pressures on the melting curve. Samples are then cooled nearly isochorically to the temperature of observation. The optical cell is equipped with sapphire windows[60,61] so that the sample may be studied *in situ* within its high pressure jacket. The method has been used in inelastic neutron scattering studies of neon[62,63] and krypton.[64] The method has the following advantages: (1) The high pressure prevents sample cracking and the resultant loss of optical quality; (2) for the same reason the external optical surfaces remain flat and of high optical quality; (3) the shifts of spectral lines with temperature directly represent temperature-dependent anharmonic self-energies; and (4) growing samples of different densities allows the determination of the volume dependence of the Raman frequencies which can then be compared to the volume dependence calculated with various anisotropic intermolecular potentials.

The pressure generating system is a standard research tool in our laboratory and has been extensively described.[65,66] The gas under investigation, in this case nitrogen, is used as the pressure transmitting fluid. Prepressurization is accomplished by a 2 kbar air-operated pump. The main valve is closed and the pressure is further increased using an intensifier with an area ratio of 15:1. The intensifier piston is driven by a hand-operated oil pump. The pressure is transmitted to the optical cell and pressure gauge through hard drawn stainless steel pressure tubing. In this manner, pressures of 10 kbar are easily reached. Pressure is measured by a high precision manganin gauge constructed and calibrated in this laboratory.[65] Pressures measured with this gauge are estimated to be accurate to better than 5 bars in the 0–10 kbar range.

The high pressure optical cell used in this study has been designed by one of the authors (WBD) and will be described elsewhere. It is constructed from maraging steel and has an estimated bursting pressure well above 10 kbar. It is attached to the cold finger of a cryostat capable of operation at liquid helium temperature. Two radiation shields and a vacuum jacket are placed around the cell.

The temperature is controlled to better than 0.1 °K by a Kelvin resistance bridge arrangement having a temperature sensor as one arm and a variable resistance as the balance arm. When the bridge is not balanced,

TABLE III. Melting parameters and phases studied.

Sample	Melting temperature (°K)	Melting pressure (kbar)	Molar volume of solid (cm^3/mole)	Phases studied
1	112 ± 0.2	2.85 ± 0.02	26.94 ± 0.06	β, α
2	131 ± 0.2	4.28 ± 0.02	26.00 ± 0.06	β, α
3	151 ± 0.2	6.00 ± 0.02	25.15 ± 0.06	β, α
4	189 ± 0.2	9.75 ± 0.02	23.75 ± 0.06	β, γ
5,6	125 ± 0.2	3.80 ± 0.02	26.30 ± 0.06	α

the amplified error signal activates either the heaters or a valve that allows the flow of coolant around the cold finger, depending on whether the cold finger is too cold or too hot. Four terminal platinum and germanium thermometers are used to measure the temperature above and below 40 °K, respectively. The resistances of the sensors are measured by a Müeller bridge with a reversing mercury switch. In this manner, temperatures can be measured to ± 0.1 °K.

Nitrogen gas from the Matheson Gas Co. of a stated minimum purity of 99.9995% was used to grow samples of the high temperature β phase at several points on the melting curve, depending on which phase was to be studied at low temperatures. Figure 1 was used as a guide and the corresponding melting parameters were then determined from Cheng's data.[15] To grow a particular sample the temperature was maintained constant while the pressure was slowly increased until the solid began to grow. A heating wire was wound around the pressure tubing near the optical cell to prevent the nitrogen from freezing and blocking the tubing. In order to prevent the solid from growing near the pressure inlet another heater was placed on a pressure fitting, maintaining a temperature difference of ~1 °K across the cell. This temperature difference introduced density differences across the samples of less than 0.1%. Samples were grown in periods of up to 12 h and then annealed overnight to remove density gradients. Each sample was then cooled through the β phase and into the α or the γ phase. Table III contains a summary of the samples grown, indicating the melting pressure and temperature, the molar volume of the solid and the phases studied.

The molar volume of each sample remained essentially constant during the entire run since it is constrained within the optical cell. However, changes in volume of the cell due to changes in temperature and pressure have been estimated using elasticity theory,[67] and Benson's[66] expressions for the volume thermal expansion coefficient, and the modulus of elasticity in tension for maraging steel. Table IV summarizes the corrected molar volumes and estimated errors for samples 1–4 at four different temperatures. These values have been used to trace the path that each sample takes during each run, shown in Fig. 1. For samples 5 and 6 which were grown to study the temperature dependence of the Raman frequencies and linewidths in the α phase, the corrected molar volumes at 40 and 5 °K are 26.18 and 26.17 cm^3/mole, respectively.

The Raman spectra were excited by the 5145 Å line of an argon-ion laser in the usual 90° scattering geometry. The 4880 Å line was used occasionally as a check. The scattered light was analyzed with a Chromatix DS-40 double monochromator with Bausch and Lomb 1800 lines/mm gratings, blazed at 5000 Å. It was detected and displayed by a Channeltron photomultiplier and a photon counting system with output to a chart recorder.

III. RESULTS AND DISCUSSION

A. Raman spectrum in the γ phase

Sample 4 became nearly opaque when taken into the γ phase in the sense that in the 1 cm long sample essentially the entire exciting beam was attenuated by intergranular anisotropies of the polycrystalline sample. The Raman spectrum of γ-N_2 in Fig. 3 was taken at 8 °K and about 5 kbar and shows two lines in the lattice region with frequencies of 58.4 and 103.6 cm^{-1}. These frequencies are in good agreement with those measured by Thiery *et al.*,[23] contrary to the conclusion of Luty and Pawley[68] who did not realize that our sample was grown at 9.75 kbar and cooled nearly "isochorically," not isobarically, to the γ phase. The lattice region was scanned from 25 to 200 cm^{-1}, revealing no additional spectral features. However, because of the large amount of elastically scattered light it was difficult to scan within 25 cm^{-1} of the laser line. A shoulder was observed on the elastic peak around 20 cm^{-1} which could not be resolved. However, this shoulder is located at the base of the laser line more than seven orders of magnitude be-

TABLE IV. Corrected molar volumes in cm^3/mole.

Samples and melting parameters / T(°K)	Sample 1 112 °K 2.85 kbar 26.94 cm^3/mole	Sample 2 131 °K 4.28 kbar 26.00 cm^3/mole	Sample 3 151 °K 6.00 kbar 25.15 cm^3/mole	Sample 4 189 °K 9.75 kbar 23.75 cm^3/mole
55	26.87 ± 0.08	25.90 ± 0.09	25.05 ± 0.09	23.59 ± 0.10
33	26.84 ± 0.08	25.88 ± 0.09	25.02 ± 0.09	23.56 ± 0.10
18	26.83 ± 0.08	25.87 ± 0.09	25.01 ± 0.09	23.55 ± 0.10
8	26.82 ± 0.08	25.87 ± 0.09	25.00 ± 0.09	23.55 ± 0.10
Change from melting curve to 8 °K	0.4%	0.5%	0.6%	0.9%

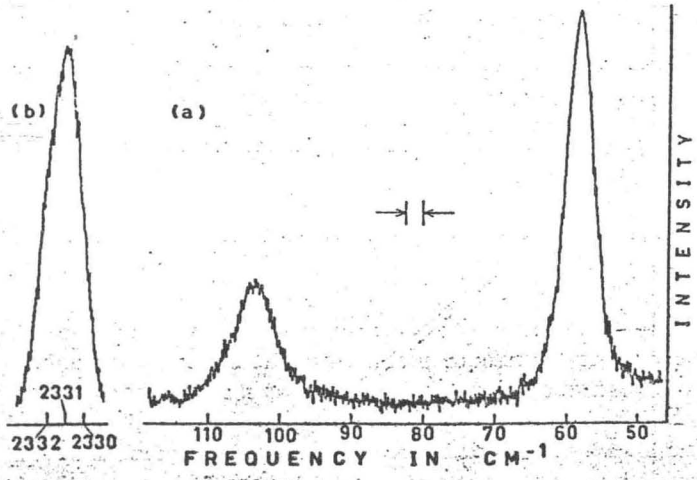

FIG. 3. Raman spectrum of the γ phase at 8 °K: (a) lattice region; (b) stretching region.

low the peak and is possibly part of the instrumental profile made visible by the extreme elastic scattering from the sample. Figure 3 also shows an asymmetrical line in the stretching region with a frequency of 2331 cm^{-1}. Table V shows the results for different temperatures.

The librational frequencies calculated in the harmonic approximation including quadrupolar interactions to 12th nearest neighbors are $\omega(E_g) = 42$ cm^{-1} and $\omega(B_{1g}) = 82$ cm^{-1}. A calculation of the relative intensities for polarized incident light in the usual 90° scattering geometry yields the ratio 1.8:1 favoring the E_g mode.[69] On the basis of these calculations the low and high frequency Raman lines are assigned to librational modes of E_g and B_{1g} symmetry, respectively.[58] The poor agreement between calculated and measured frequencies is to be expected since, at the higher densities corresponding to the γ phase, the repulsive part of the potential becomes more important. Calculations using the 6–12[38] and 6–exp[68] atom–atom potentials are in good agreement with experiment.

The strong temperature dependence of the B_{1g} librational frequency seems to point to a softening of this mode as the γ to β transition is approached. In going to the β phase, where the molecular centers are arranged in an hcp structure, the square faces of the unit cell of γ–N_2 shown in Fig. 2 have to be sheared. The B_{1g} librational mode, which corresponds to librations in the plane of the square faces, can then become soft through coupling to the infrared active E_u translational mode that corresponds to the shearing motion.

TABLE V. Observed Raman frequencies and relative intensities for the γ phase.

Temperature	Frequency (cm^{-1})	Relative integrated intensity
	57.5	2
35 °K	95.5	4.5
	2329	1
	58.2	5.5
20 °K	102.5	3
	2330	1
	58.4	7
8 °K	103.6	2.5
	2331	1

B. Volume dependence of the Raman frequencies in the α phase

Figure 4 shows the Raman spectrum in the lattice region of the α phase. Three sharp lines are observed corresponding to librations of E_g, T_{2g}, and T_g symmetry, in agreement with previous results.[19–23] In addition, a broad band is observed from about 70 to 100 cm^{-1}. In the stretching region, not shown in Fig. 4, two lines with a separation of about 1.2 cm^{-1} have been resolved.

Samples 1–3 were grown to study the volume dependence of the Raman frequencies in the α phase. The results for these samples are summarized in Table VI. Because of broadening, only the frequency of the E_g line could be determined at 33 °K. The frequencies increase with decreasing molar volumes, while the full widths at half intensity seem to be independent of volume.

The lattice frequencies are independent of volume and temperature in the harmonic approximation. In the quasiharmonic approximation[70] the frequencies are dependent on volume. Usually the dominant quasiharmonic contribution to the volume dependence arises because of a shift in the point of evaluation of the second order force constants used in a harmonic calculation. A measure of the volume dependence of the normal mode frequencies $\omega(j)$ is given by the Grüneisen parameter of the jth mode

$$\gamma_j = (-\partial \ln\omega(j)/\partial \ln V)_T , \qquad (1)$$

where V is the molar volume. These parameters are critically dependent on the form of the intermolecular

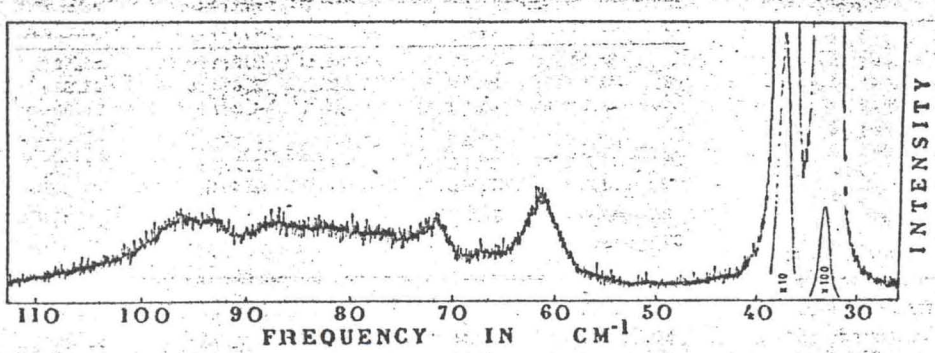

FIG. 4. Raman spectrum in the lattice region of the α phase for a sample with a molar volume of 26.82 cm^3/mole at 8 °K. Instrumental resolution is 1 cm^{-1}.

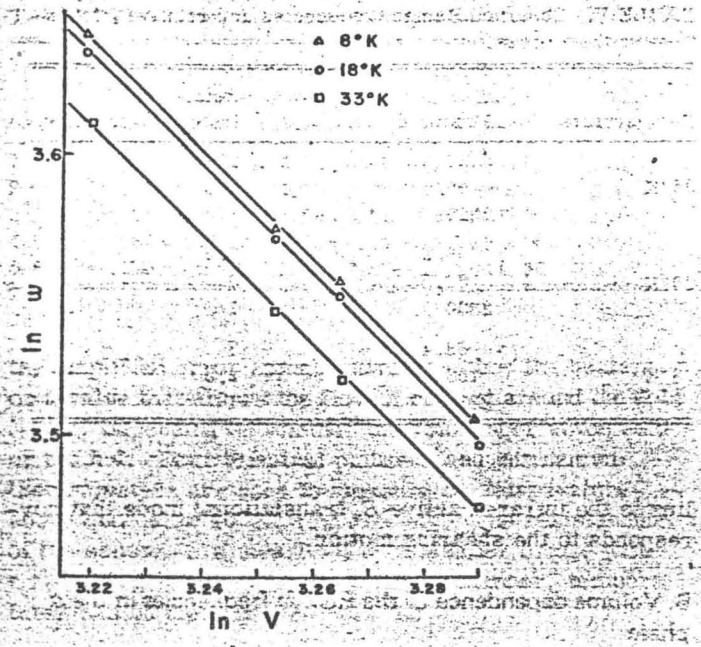

FIG. 5. Plot of $\ln\omega$ versus $\ln V$ for the E_g mode of the α phase, where the frequency ω is in cm^{-1} and the molar volume V is in cm^3/mole: ×, experimental points; ——, best fit to a straight line.

potential, especially the short-range repulsive part.

The Grüneisen parameters for the librational modes were obtained using the data in Table VI. In Figs. 5–7, constructed from this data, $\ln\omega$ is plotted versus $\ln V$ for each of the modes. Also shown in Fig. 5 are data points for the E_g mode from sample 6. The data points were fitted to a straight line, shown by solid lines in the figures. The negative slope of each line is the Grüneisen parameter for that particular mode. The Grüneisen

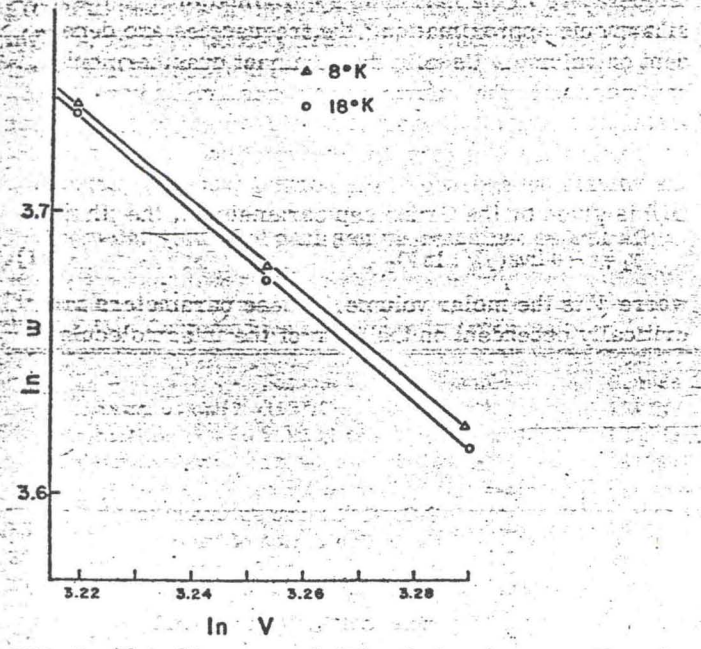

FIG. 6. Plot of $\ln\omega$ versus $\ln V$ for the low-frequency T_g mode of the α phase, where the frequency ω is in cm^{-1} and the molar volume V is in cm^3/mole: ×, experimental points; ——, best fit to a straight line.

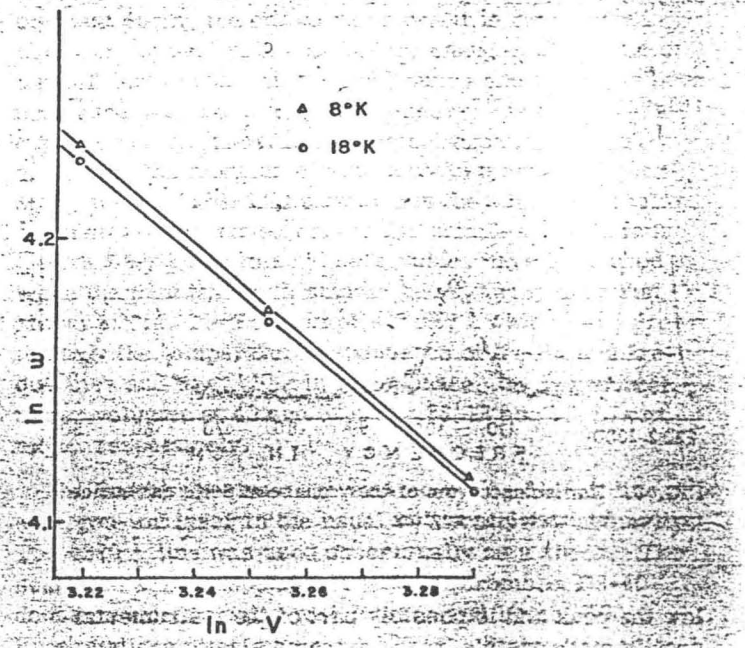

FIG. 7. Plot of $\ln\omega$ versus $\ln V$ for the high-frequency T_g mode of the α phase, where the frequency ω is in cm^{-1} and the molar volume V is in cm^3/mole: ×, experimental points; ——, best fit to a straight line.

parameters and estimated errors were determined using a least square fit. The results are summarized in Table VII. The measured Grüneisen parameters are independent of temperature within the experimental errors. They are substantially higher than the result of $\frac{5}{6}$ expected for a quadrupolar interaction potential in the quasiharmonic approximation. This result of $\frac{5}{6}$ follows from the relation $\omega^2 \propto r^{-5}$ between the librational frequency ω and the intermolecular distance r. The spectroscopic values are closer to the value $1.0 \leq \gamma \leq 1.5$ obtained by Brookeman, McEnman, and Scott[39] using nuclear quadrupole resonance methods.

Zunger and Huler[36] used a 6–12 atom–atom potential and obtained Grüneisen parameters around 3 for the librational modes of the α phase. Raich, Gillis, and Anderson[49] used this potential in a self-consistent calculation and obtained Grüneisen parameters 15%–50%

TABLE VI. Volume dependence of the Raman spectrum in the α-phase.

T (°K)	Frequency (full width at half-intensity) (cm^{-1}) E_g	T_g	T_g	Relative peak intensities $E_g:T_g:T_g$	Molar volume (cm^3/mole)
8	33.3[a]	37.5[a]	61.3(4.5)	3.6:1:0.05	26.82
	35.6(0.8)	39.7(0.8)	65.0(5)	3.6:1:0.05	25.87
	38.2(0.8)	42.0(0.8)	69.0(5)	4.2:1:<0.05	25.00
18	33.0(1.7)	37.2(1.7)	61.0(5.5)	4.7:1:0.05	26.83
	35.5(1.7)	39.5(1.7)	64.8(6)	5.2:1:<0.05	25.87
	38.0(1.7)	41.9(1.7)	68.6(6)	5.5:1:<0.05	25.01
33	32.3(8)	...	...	...	26.84
	34.6(8)	...	...	...	25.88
	37.0(8)	...	...	...	25.02

[a]These lines are very narrow and the linewidths cannot be resolved from the instrumental widths.

TABLE VII. Grüneisen parameters for the librational modes in the α phase.

T (°K)	E_g mode	Low-frequency T_g mode	High-frequency T_g mode
8	1.95±0.06	1.63±0.06	1.68±0.08
18	1.95±0.06	1.68±0.06	1.65±0.08
33	1.96±0.08		

larger than the measured values. These results seem to indicate that the 12 power of the repulsive part is too high. Indeed, for a repulsive atom–atom potential of the form Ar^{-n}, the Grüneisen parameters obtained in the present study would yield $9.3<n<10.1$ and $7.4<n<8.4$ for the E_g and T_g modes, respectively, in the quasi-harmonic approximation. This conclusion is substantiated by the classical harmonic calculations of Jacobi and Schnepp,[47] who used the 6–n atom–atom potential and found $n=9$ to give better agreement with the measured lattice energy, and infrared and Raman frequencies at zero pressure. Using a multipole expansion of the intermolecular potential Mandell[50] obtained Grüneisen parameters of about 2 and 1.7 for the E_g and two T_g modes, respectively. However, the author's assumption of a hexadecapole–monopole term independent of volume is not fully justified.[50]

The measured librational frequencies can be extrapolated to zero pressure using the Grüneisen parameters and the molar volumes at zero pressure from Fig. 1. The calculated zero pressure librational frequencies are 32.8, 37.0, and 60.5 cm^{-1} at 8 °K and 32.3, 36.6, and 60.1 cm^{-1} at 18 °K to be compared to 31.5, 36.0, and 59.8 cm^{-1} measured by Mathai and Allin[22] at 4 °K and 32, 36.5, and 60 cm^{-1} measured by Anderson, Sun, and Donkersloot[21] at 18 °K.

The band between 70 and 100 cm^{-1} in Fig. 4 seems to consist of a series of broad lines, the most pronounced being around 70 and 95 cm^{-1}. These frequencies are close to the sum of the E_g and each of the T_g librational modes, indicating that it might be a two-libron band. However, the 70 cm^{-1} line could coincide with an infrared-active phonon.[24–26] To check these possibilities, the Grüneisen parameters of both lines at 8 °K were estimated to be 2.2 and 2.0, respectively. These values are close to those obtained for the librational modes and favors its identification as a two-libron band, as previously suggested.[46]

The individual Grüneisen parameters are related to the Grüneisen gamma γ_G and other thermodynamic functions by

$$\frac{1}{C_V}\sum_j \gamma(j)C_{Vj}=\gamma_G=\frac{\alpha V}{C_V K_T}\,, \tag{2}$$

where C_{Vj} and C_V are the heat capacity at constant volume for the jth mode and the solid, respectively; α is the volume coefficient of thermal expansion; and K_T is the isothermal compressibility. Heberlein, Adams, and Scott[15] calculated γ_G using experimental values of the other thermodynamic functions in Eq. (2). They obtained a γ_g strongly temperature dependent above 16 °K, leveling off to a value around 3 just below the α–β transition. Since the Grüneisen parameters for the librational modes are substantially lower than three, it must be concluded that these modes cannot be responsible alone for the increase in γ_G. Translational modes probably having Grüneisen parameters around 3 must make significant contributions to γ_g below 36 °K.

C. Temperature dependence of E_g librational frequency in the α phase

In an isobaric experiment, the changes in the librational frequencies with temperature contain one contribution due to thermal expansion and a second contribution which is a direct result of anharmonic interactions and is present even in a solid held at constant volume. This last contribution has been measured in samples five and six. The change in molar volume of these "clamped" samples in the temperature range 5–39 °K introduces a change in the E_g librational frequency of about 0.05 cm^{-1}. This change is considerably less than the errors in the frequencies and it is reasonable to assume that the Raman spectrum in the α phase for these samples is only directly affected by changes in temperature. The E_g librational frequencies of these samples are given in Table VIII at intervals of about 3 °K in the temperature range 5–39 °K.

Although the librational amplitudes are large in the α phase, Harris and Coll[46] have shown that they are small enough to warrant a perturbation treatment starting from conventional lattice dynamics. This treatment has been widely considered in the literature in the case of translational modes. For an extensive discussion on the subject the reader is referred to Wallace's book.[71] Usually, cubic and quartic anharmonic terms are added to the potential and the total energy is then calculated in second-order perturbation. The resulting correction to the harmonic energy is called the anharmonic self-energy. This self-energy is complex and is written as

$$\hbar\Delta\omega(\lambda)=\hbar\Delta(\lambda)-i\hbar\Gamma(\lambda)\,, \tag{3}$$

where λ refers to a mode with a particular wavevector and polarization. The quantity $\Delta(\lambda)$ represents the shift in the phonon frequency and $2\Gamma(\lambda)$ is the full width at

TABLE VIII. Temperature dependence of the frequency and linewidth of the E_g line in the α phase.

Sample 5			Sample 6		
T (°K)	Frequency (cm^{-1})	Full width at half-intensity (cm^{-1})	T (°K)	Frequency (cm^{-1})	Full width at half-intensity (cm^{-1})
38.6	32.5±0.3	10.0(12.0)	38.9	32.5±0.3	9.7(12.6)
35.9	33.1±0.3	8.5(10.4)	36.0	33.1±0.3	8.0(10.8)
32.9	33.7±0.3	6.5(8.4)	32.9	33.7±0.3	6.3(9.0)
29.8	34.1±0.2	5.0(6.6)	29.4	34.0±0.2	4.7(7.4)
26.9	34.4±0.2	3.7(5.1)	26.8	34.3±0.2	3.7(6.2)
24.6	34.5±0.2	2.7(4.2)	24.2	34.6±0.2	2.8(5.0)
21.0	a	1.8(2.6)	20.9	34.8±0.1	1.9(3.2)
17.0	a	0.8(1.6)	17.1	34.9±0.1	1.0(2.2)
12.7	34.95±0.1	0.4(1.2)	12.7	34.95±0.1	0.3(1.2)
9.8	34.95±0.1	0.2(0.9)	9.7	35.0±0.1	0.2(0.9)
5.0	35.0±0.1	0.1(0.6)	5.0	35.0±0.1	0.1(0.6)

[a]These frequencies could not be obtained owing to irregularities in the chart recorder.

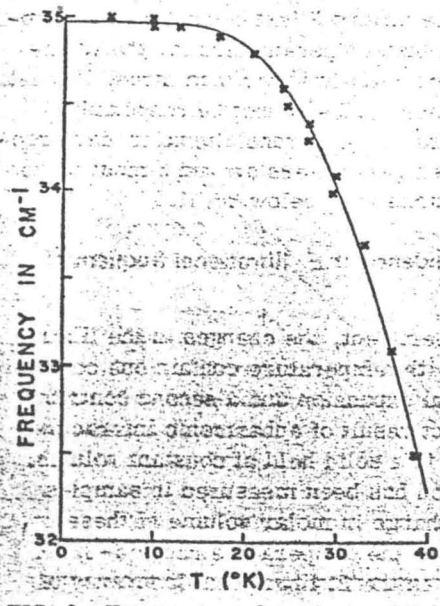

FIG. 8. Temperature dependence of the E_g librational frequency of the α phase: ×, experimental points from samples five and six; ——, best fit to the function in (6).

half-intensity of the corresponding Raman line. In second-order perturbation both cubic and quartic anharmonic terms contribute to $\Delta(\lambda)$ while only cubic terms contribute to $\Gamma(\lambda)$.

The frequency shift is given by[71]

$$\Delta(\lambda) = C(\lambda) + \sum_{\lambda'} C(\lambda, \lambda')\, n(\lambda'), \tag{4}$$

where $C(\lambda)$ and $C(\lambda, \lambda')$ are temperature independent factors depending only on the strengths of the cubic and quartic anharmonic interactions and on the crystal configuration. The factor $n(\lambda')$ is the average occupation number given by

$$n(\lambda') = \{\exp[\hbar\omega_0(\lambda')/kT] - 1\}^{-1}, \tag{5}$$

where $\omega_0(\lambda')$ refers to the harmonic frequency. For the simple case when the E_g libron strongly interacts only with one other excitation, the E_g frequency can be written as

$$\omega(E_g) = \omega_1(E_g) + \omega_2(E_g)\{\exp[\hbar\omega_0(\lambda')/kT] - 1\}^{-1}. \tag{6}$$

The data points from Table VIII were fitted to a function of the form given by (6). The best fit, shown in Fig. 8 by the solid line, was obtained with $\omega_1(E_g) = 34.97\ \text{cm}^{-1}$, $\omega_2(E_g) = -51.9\ \text{cm}^{-1}$, and $\omega_0(\lambda') = 83\ \text{cm}^{-1}$. The error in the frequency $\omega_0(\lambda')$ was estimated at $\pm 12\ \text{cm}^{-1}$.

This characteristic frequency around 83 cm^{-1} seems too high to represent the excitation of other *librons* to interact with the E_g libron. A more reasonable explanation is that the E_g librons are interacting with phonons. In particular, the infrared-active T_u phonon with an anomalous width has a zero pressure frequency of 70 cm^{-1} which, when extrapolated to a molar volume of 26.2 cm^3/mole assuming a Grüneisen gamma of 3, results in a frequency of 77 cm^{-1}. This value is close to 83 cm^{-1}, indicating that the frequency dependence of the E_g line can be explained if the E_g librons are interacting only with T_u phonons through quartic anharmonicity. It should be mentioned at this point that Mandell[50] has shown that libron–phonon interactions have an important effect in the multipole expansion of the anisotropic intermolecular potential.

The quadrupolar interaction potential has been used in Monte Carlo calculations for classical free rotors[48] resulting in qualitatively the wrong temperature dependence for the librational frequencies in the α-phase. Self-consistent calculations[49] with a 6–12 atom–atom potential yield the correct temperature dependence but the calculated frequency changes are substantially lower than the measured changes.

At this point, a brief excursion is taken back to γ-N_2 and the strong temperature dependence of the B_{1g} frequency. The B_{1g} frequencies were fitted to the function given in (6), resulting in a characteristic frequency $\omega_0(\lambda') = 62\ \text{cm}^{-1}$. Although the fit is inaccurate due to the small number of data points, it would be interesting to measure the frequency of the infrared active E_u phonon. However, theoretical calculations[36,68] result in E_u frequencies of 64.4 and 66.1 cm^{-1} at 4 and 4.5 kbar, indicating that the B_{1g} librons might indeed couple to E_u phonons.

D. Temperature dependence of the linewidth of the E_g line in the α phase

The true linewidth of the E_g line in the α phase is given in Table VIII at several temperatures. The linewidth in (not in) parentheses were obtained assuming that both the instrumental profiles and the true line shape are given by Gaussian (Lorentzian) curves.

The imaginary part of the self-energy in Eq. (3), which is related to the linewidth of a Raman line, is given by[71]

$$\Gamma(\lambda) = \frac{18\pi}{\hbar^2} \sum_{\lambda'\lambda''} |\phi(\lambda, \lambda', \lambda'')|^2 \{[n(\lambda') + n(\lambda'') + 1]\,\delta[\omega_0(\lambda) - \omega_0(\lambda') - \omega_0(\lambda'')]$$
$$+ [n(\lambda') - n(\lambda'')][\delta(\omega_0(\lambda) + \omega_0(\lambda') - \omega_0(\lambda'')) - \delta(\omega_0(\lambda) - \omega_0(\lambda') + \omega_0(\lambda''))]\}, \tag{7}$$

where $\phi(\lambda, \lambda', \lambda'')$ is related to the cubic anharmonic term in the potential. Wallis, Ipatova, and Maradudin[72] also considered quartic anharmonic contributions in higher-order perturbation. Their result has been simplified by Gervais, Piriou, and Cabannes,[73] who assumed that the phonon under investigation decays into two or three phonons having frequencies which are dispersed around an average. The result is given by

$$\Gamma(\lambda) = \Gamma_1(\lambda)[n(\omega_1) + \tfrac{1}{2}] + \Gamma_2(\lambda)\{[n(\omega_2) + \tfrac{1}{2}]^2 + \tfrac{1}{12}\}, \tag{8}$$

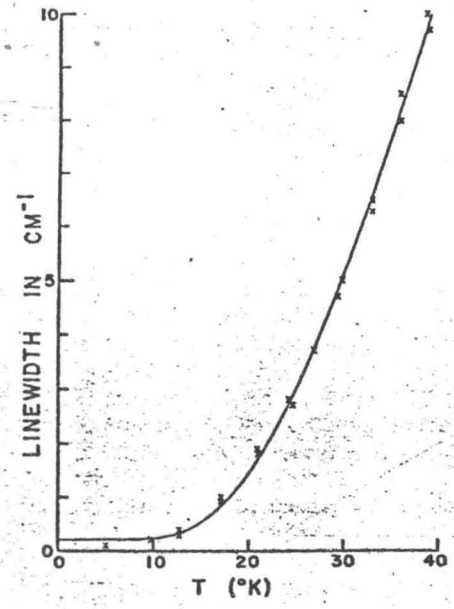

FIG. 9. Temperature dependence of the true linewidth of the E_g line of the α phase: ×, experimental points obtained assuming that both the true line and the instrumental profile are given by Lorentzian curves; ——, best fit to the function in Eq. (9).

where $\omega_1 = \frac{1}{2}\omega_0(\lambda)$ and $\omega_2 = \frac{1}{3}\omega_0(\lambda)$, and $\Gamma_1(\lambda)$ and $\Gamma_2(\lambda)$ are temperature independent.

The linewidths from Table VIII were fitted to the function given in (8), but both sets of values resulted in extremely poor fits. The difficulty arising in these fits seems to be the smallness of the linewidth at very low temperatures. This is easily resolved by considering the second term in (7). This term will go to zero at 0 °K. Then, the small linewidth observed at 5 °K can be attributed to other less important anharmonic interactions.

If there is one dominant cubic anharmonic interaction that allows the E_g libron to combine with a second excitation to produce a third, Eq. (7) becomes

$$\Gamma(\lambda) = \Gamma_1(\lambda) + \Gamma_2(\lambda)\,[n(\omega') - n(\omega + \omega')] \qquad (9)$$

where ω, ω', and $\omega'' = \omega + \omega'$, refer to the frequencies of the E_g libron and the other two excitations, respectively. The term $\Gamma_1(\lambda)$ has been added to account for the small linewidth near 0 °K.

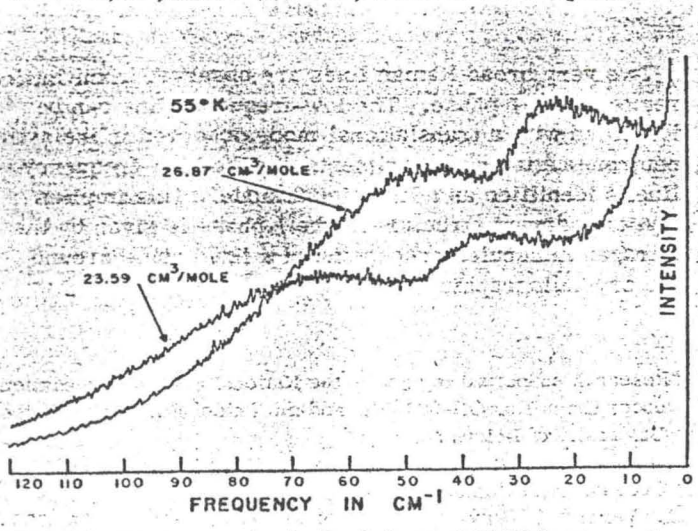

FIG. 10. Raman spectra in the β phase at 55 °K from samples with molar volumes of 23.59 and 26.87 cm³/mole. Instrumental resolution is 2 cm⁻¹.

TABLE IX. Volume dependence of Raman frequencies in the β phase at 55 °K.

Sample	Molar volume (cm³/mole)	Frequencies (cm⁻¹)	
1	26.87	25±3	50±3
2	25.90	28±3	54±3
3	25.05	31±3	58±3
4	23.59	36±3	68±3

The two sets of linewidths were fitted to the function given in equation (9) with $\omega = 35$ cm⁻¹. Figure 9 shows the best fit for the set of linewidths not in parentheses in Table VIII. The resulting parameters are $\Gamma_1(\lambda) = 0.2$ cm⁻¹, $\Gamma_2(\lambda) = 140$ cm⁻¹, $\omega' = 63$ cm⁻¹, $\omega'' = 98$ cm⁻¹; and $\Gamma_1(\lambda) = 0.6$ cm⁻¹, $\Gamma_2(\lambda) = 106$ cm⁻¹, $\omega' = 54$ cm⁻¹, $\omega'' = 89$ cm⁻¹. The errors in these results are probably large and difficult to estimate. However, they show that the process responsible for the temperature dependence of the linewidth of the E_g line is possibly a combination with a T_g libron to create a T_u phonon. The reverse process of a T_u phonon decaying into E_g and T_g librons has been proposed as an explanation for the anomalous width of the infrared-active T_u phonon with a zero pressure frequency of 70 cm⁻¹.[48] Although the characteristic frequencies ω' and ω'' are larger than those corresponding to the low-frequency T_g libron and the infrared-active T_u phonon in samples 5 and 6, the discrepancies might be due to the failure to consider other less important anharmonic processes.

The coefficient $\Gamma_2(\lambda)$ can be related to the cubic anharmonic term H_3 in the Hamiltonian. Using $\Gamma_2(\lambda) = 120$ cm⁻¹ results in $|H_3|^2 \simeq 1.2(\text{cm}^{-1})^2$ in good agreement with the value of about $1(\text{cm}^{-1})^2$ estimated by Harris and Coll[46] for the cubic anharmonic interaction which allows the infrared-active T_u phonon to decay into two librons.

E. β phase

Figure 10 shows Raman spectra in the lattice region of the β phase for samples one and four at 55 °K. Two extremely broad lines are seen, whereas previous workers observed only a wing on the Rayleigh line.[20] Indeed, the high-frequency tail of the spectrum resembles the wing of the Rayleigh line in the fluid phase. In the stretching region, not shown in the figure, a single line is observed having a wing on each side. Table IX summarizes the results for samples one to four at 55 °K. These frequencies are obtained by fitting Gaussian curves after subtracting a background having the shape of the Rayleigh wing in the fluid and drawn to fit the high-frequency tail of the spectrum in the β phase. Table X shows the temperature dependence of the Raman frequencies for sample four.

Figure 11 shows a plot of $\ln\omega$ versus $\ln V$ for the two Raman lines of the β phase at 55 °K. The straight lines that fits the data best are shown by solid lines and result in Grüneisen parameters of 2.8±0.5 and 2.4±0.5 for the low- and high-frequency lines.

Kjems and Dolling[74] recently used inelastic neutron scattering to study the lattice dynamics of the β-phase. They observed two translational modes at $q=0$ and 36 °K having frequencies of 25 and 64 cm^{-1}. The low frequency mode splits into two modes for $q \neq 0$ and corresponds to the doubly degenerate E_{2g} mode shown in Table II. This E_{2g} mode is Raman-active and can be identified with the low-frequency line in the Raman spectrum of sample one having a frequency of 25 cm^{-1} at 55 °K. This identification is supported by the large Grüneisen parameter of this line, usually characteristic of translational modes in close-packed molecular crystals. The other translational mode observed by Kjems and Dolling at $q=0$ has too high a frequency to correspond to the other Raman line. Moreover, only one translational mode is expected in the first-order Raman spectrum of an hcp structure. The second Raman line then probably corresponds to a librational mode of E_{1g} symmetry, as expected from Table II. This means that the molecules in the β phase are precessing around the c axis.

The high-frequency Raman line could be a two-phonon band. However, this is unlikely since both Raman lines have comparable linewidths and strikingly different temperature dependences. Also, the Grüneisen parameter for this line is somewhat smaller than that of the E_{2g} phonon and closer to those obtained for the librational modes in the α phase. It should be pointed out that the measured Grüneisen parameter for this libration is, as in the α phase, much larger than the value expected for a quadrupolar interaction potential in the quasiharmonic approximation.

The temperature dependence of the frequencies in Table X was fitted to a function of the form given by (6). However, variations in the choice of the frequency at 0 °K had little effect on the fit but drastically changed the characteristic temperature, rendering any results meaningless. Also, no indication of the ordering transition without thermal anomaly suggested by Mandell[48] has been found.

IV. CONCLUSION

The Raman spectrum of the three known phases of solid nitrogen has been studied in the ranges from 0 to 220 °K and 0 to 10 kbar. A novel method is used in that each sample is grown within a high pressure optical cell which constrains it to nearly isochoric conditions. This method allows the separation of temperature and volume effects.

Two lines in the lattice region and one slightly asymmetrical line in the stretching region have been observed in the Raman spectrum of the γ phase. Comparison of experimental and calculated frequencies and relative intensities allows the identification of the low- and high-frequency lines in the lattice region as E_g and B_{1g} librational modes, respectively.

In the α phase, the measured Grüneisen parameters indicate that neither the quadrupolar nor the 6–12 atom–atom interaction potential has the correct volume dependence. The failure to observe any coincidence between the Raman and infrared frequencies supports the assignment of a $Pa3$ structure to the α phase. The temperature dependence of the E_g librational frequency can be explained if this libron is interacting mainly with a T_u phonon through quartic anharmonicity. The temperature dependence of the linewidth of the E_g mode indicates that an E_g libron is combining with another excitation (possibly a T_g libron) to create a third excitation (possibly a T_u phonon).

Two very broad Raman lines are observed in the lattice region of the β phase. The low-frequency line can be identified with a translational mode observed in inelastic neutron scattering experiments.[74] The high-frequency line is identified as a librational mode. This implies that the correct structure of the β phase is given by the nitrogen molecules precessing at a fixed angle around the crystallographic c axis.

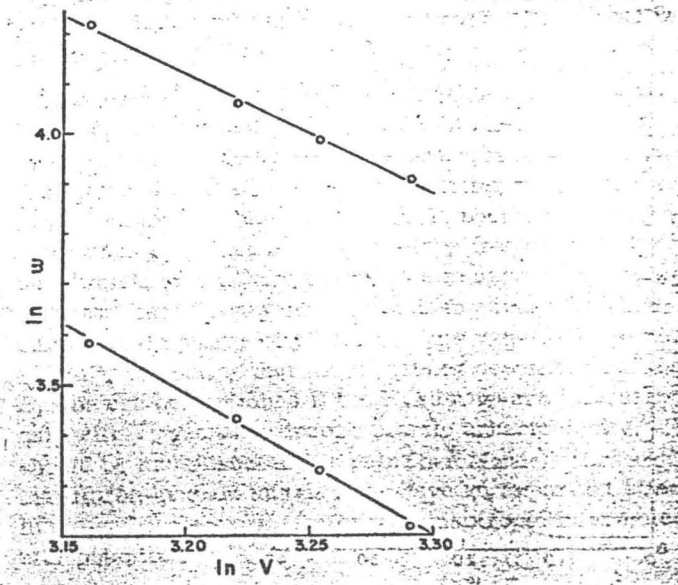

FIG. 11. Plot of $\ln\omega$ versus $\ln V$ for the two Raman lines in the β phase where the frequency ω is in cm^{-1} and the molar volume V is in cm^3/mole: ×, experimental points; ——, best fit to a straight line.

TABLE X. Temperature dependence of Raman frequencies in the β phase for sample 4.

T (°K)	Frequencies (cm^{-1})	
55	36±3	68±3
80	34±4	67±4
102	32±4	67±4
135	30±5	66±5
170	26±5	66±5

*Research supported in part by the National Science Foundation under Grant No. GH-32491-X and the Unidel Foundation of the University of Delaware.

†Present address: School of Physics, Georgia Institute of Technology, Atlanta, GA 30332.

[1]L. Vegard, Z. Phys. 58, 497 (1929); 79, 471 (1932); 88, 235 (1934).

[2]M. Ruhemann, Z. Phys. 76, 368 (1932).

[3]L. H. Bolz, M. E. Boyd, F. A. Mauer, and H. S. Peiser,

Acta Crystallogr. 12, 247 (1959).
[4]W. E. Streib, T. H. Jordan, and W. N. Lipscomb, J. Chem. Phys. 37, 2962 (1962).
[5]T. H. Jordan, H. W. Smith, W. E. Streib, and W. N. Lipscomb, J. Chem. Phys. 41, 756 (1964).
[6]A. F. Schuch and R. L. Mills, J. Chem. Phys. 52, 6000 (1970).
[7]S. J. LaPlaca and W. C. Hamilton, Acta Crystallogr. B 28, 984 (1972).
[8]E. M. Hörl and L. Marton, Acta Crystallogr. 14, 11 (1961).
[9]J. Donohue, Acta Crystallogr. 14, 1000 (1961).
[10]J. A. Venables, Philos. Mag. 21, 147 (1970).
[11]J. A. Venables and C. A. English, Acta Crystallogr. B 30, 929 (1974).
[12]C. A. Swenson, J. Chem. Phys. 23, 1963 (1955).
[13]J. W. Stewart, J. Phys. Chem. Solids 1, 146 (1956).
[14]R. L. Mills and A. F. Schuch, Phys. Rev. Lett. 23, 1154 (1969).
[15]V. M. Cheng, Ph.D. thesis, Princeton University, 1972.
[16]D. C. Heberlein, E. D. Adams, and T. A. Scott, J. Low Temp. Phys. 2, 449 (1970).
[17]J. R. Brookeman and T. A. Scott, J. Low Temp. Phys. 12, 491 (1973).
[18]D. J. Gannon and J. A. Morrison, Can. J. Phys. 51, 1590 (1973).
[19]M. Brit, A. Ron, and O. Schnepp, J. Chem. Phys. 51, 1318 (1969).
[20]J. E. Cahill and G. E. Leroi, J. Chem. Phys. 51, 1324 (1969).
[21]A. Anderson, T. S. Sun, and M.C.A. Donkersloot, Can. J. Phys. 48, 2265 (1970).
[22]P. M. Mathai and E. J. Allin, Can. J. Phys. 49, 1973 (1971).
[23]M. M. Thiery, D. Fabre, M. Jean-Louis, and H. Vu, J. Chem. Phys. 59, 4559 (1973).
[24]A. Anderson and G. E. Leroi, J. Chem. Phys. 45, 4359 (1966).
[25]A. Ron and O. Schnepp, J. Chem. Phys. 46, 3991 (1967).
[26]R. V. St. Louis and O. Schnepp, J. Chem. Phys. 50, 5177 (1969).
[27]J. R. Brookeman and T. A. Scott, Acta Crystallogr. B 28, 983 (1972).
[28]E. J. Watchell, J. Chem. Phys. 57, 5620 (1972).
[29]O. Nagai and T. Nakamura, Prog. Theor. Phys. (Kyoto) 24, 432 (1960).
[30]B. Kohin, J. Chem. Phys. 33, 882 (1960).
[31]J. Felsteiner, Phys. Rev. Lett. 15, 1025 (1965).
[32]J. Felsteiner, D. B. Litvin, and J. Zak, Phys. Rev. B 3, 2706 (1971).
[33]J. Felsteiner and Z. Friedman, Phys. Rev. B 8, 3996 (1973).
[34]T. Kuan, A. Warshel, and O. Schnepp, J. Chem. Phys. 52, 3012 (1970).
[35]D. A. Goodings and M. Henkelman, Can. J. Phys. 49, 2898 (1971).
[36]A. Zunger and E. Huler, J. Chem. Phys. 62, 3010 (1975).
[37]V. G. Manzhelii, A. M. Tolkachev, and E. I. Voitovich, Phys. Status Solidi 13, 351 (1966).
[38]M. I. Bagatskii, V. A. Kucheryavy, M. G. Manzhelii, and V. A. Popov, Phys. Status Solidi 26, 453 (1968).
[39]J. R. Brookeman, M. M. McEnnan, and T. A. Scott, Phys. Rev. B 4, 3661 (1971).
[40]O. Schnepp and A. Ron, Discuss. Faraday Soc. 48, 26 (1969).
[41]M. C. Donkersloot and S. H. Walmsley, Mol. Phys. 19, 183 (1970).
[42]J. C. Raich and R. D. Etters, J. Low Temp. Phys. 7, 449 (1972).
[43]J. C. Raich, J. Chem. Phys. 56, 2395 (1972).
[44]N. Jacobi and O. Schnepp, J. Chem. Phys. 57, 2516 (1972).
[45]P. V. Dunmore, J. Chem. Phys. 57, 3348 (1972).
[46]A. B. Harris and C. F. Coll III, Solid State Commun. 10, 1029 (1972).
[47]N. Jacobi and O. Schnepp, J. Chem. Phys. 58, 3647 (1973).
[48]M. J. Mandell, J. Chem. Phys. 60, 1432 (1974); 60, 4880 (1974).
[49]J. C. Raich, N. S. Gillis, and A. B. Anderson, J. Chem. Phys. 61, 1399 (1974).
[50]M. J. Mandell, J. Low Temp. Phys. 17, 169 (1974), and preprint.
[51]W. G. Fately, F. R. Dollish, N. T. McDevitt, and F. F. Bentley, *Infrared and Raman Selection Rules for Molecular and Lattice Vibrations* (Wiley, New York, 1972).
[52]J. C. Raich and R. L. Mills, J. Chem. Phys. 55, 1811 (1971).
[53]J. C. Raich, N. S. Gillis, and T. R. Koehler, J. Chem. Phys. 61, 1411 (1974).
[54]L. A. K. Staveley, J. Phys. Chem. Solids 18, 46 (1961).
[55]W. F. Lewis, R. K. Crawford, and W. B. Daniels, J. Phys. Chem. Solids 35, 1201 (1974).
[56]A. S. DeReggi, P. C. Canepa, and T. A. Scott, J. Mag. Res. 1, 144 (1969).
[57]I. F. Silvera, W. N. Hardy, and J. P. McTague, Phys. Rev. B 5, 1578 (1972).
[58]F. D. Medina and W. B. Daniels, J. Chem. Phys. 59, 6175 (1973).
[59]F. D. Medina and W. B. Daniels, Phys. Rev. Lett. 32, 167 (1974).
[60]E. Fishman and H. G. Drickamer, Anal. Chem. 28, 804 (1956).
[61]W. B. Daniels (unpublished).
[62]J. A. Leake, W. B. Daniels, J. Skalyo, Jr., B. C. Frazer, and G. Shirane, Phys. Rev. 181, 1251 (1969).
[63]J. Skalyo, Jr., V. J. Minkiewicz, G. Shirane, and W. B. Daniels, Phys. Rev. B 6, 4766 (1972).
[64]W. B. Daniels, G. Shirane, B. C. Frazer, H. Umebayashi, and J. A. Leake, Phys. Rev. Lett. 18, 548 (1967).
[65]R. K. Crawford, Ph.D. thesis, Princeton University, 1968.
[66]D. A. Benson, Ph.D. thesis, Princeton University, 1968.
[67]R. J. Roark, *Formulas for Stress and Strain* (McGraw-Hill, New York, 1954), p. 264.
[68]T. Luty and G. S. Pawley, Chem. Phys. Lett. 28, 593 (1974).
[69]This result was erroneously reported in Ref. 58 by a factor of 2.
[70]J. C. Slater, *Introduction to Chemical Physics* (McGraw-Hill, New York, 1939), pp. 215–220.
[71]D. C. Wallace, *Thermodynamics of Crystals* (Wiley, New York, 1972).
[72]R. F. Wallis, I. P. Ipatova, and A. A. Maradudin, Fiz. Tverd. Tela 8, 1064 (1966) [Sov. Phys.–Solid State 8, 850 (1966)].
[73]F. Gervais, B. Piriou, and F. Cabannes, J. Phys. Chem. Solids 34, 1785 (1973).
[74]J. K. Kjems and G. Dolling, Phys. Rev. B 11, 1639 (1975), and private communication.